Compatibilization of Polymer Blends by Complexation. 3. Structure Pinning during Phase Separation of Ionomer/Polyamide Blends

Yi Feng,[†] R. A. Weiss,*[,†] and C. C. Han[‡]

Institute of Materials Science, University of Connecticut, Storrs, Connecticut 06269-3136, and Polymers Division, National Institute of Standards and Technology, Gaithersburg, Maryland 20899

Received January 17, 1996; Revised Manuscript Received March 20, 1996[⊗]

ABSTRACT: The effects of strong intermolecular interactions on the phase behavior and phase separation kinetics of an ionomer/polyamide blend were investigated by light scattering and optical microscopy. The lithium salt of lightly sulfonated polystyrene (Li-SPS) ionomers (4.0−9.5 mol % sulfonation) and poly(*N,N′*-dimethylethylene sebacamide) (mPA) are miscible as a result of the formation of an ion−amide complex. The blends exhibit LCST-type phase behavior. Phase separation can be thermally induced and is thermodynamically reversible. The phase separation process stalls after a couple of hours due to structure pinning, which may be due to concentration of the ion−amide complexes in a ionomer-rich phase and/or the formation of microphase-separated ionic aggregates in the ionomer-rich phase.

Introduction

The properties of polymer blends are intimately tied to their morphology, which depends on the miscibility of the components and the mechanism and kinetics of phase separation. For some applications, phase-separated morphologies are required for improving mechanical properties such as impact toughness,[1] while in other instances, a miscible blend is desired, e.g., for improving processability or extending an expensive material with a cheaper one.[2] For either a single-phase or two-phase blend, the development of the optimum morphology and properties requires knowledge of the phase diagram and the characteristics of the phase separation process.

Recently, compatibilization of polymer blends by promoting intermolecular complexation has attracted considerable interest.[3] Intermolecular complexation, such as hydrogen bonding, proton transfer, transition metal coordination, or ion−dipole interaction, can result in miscible or partially miscible blends of otherwise immiscible polymers. The major emphasis of previous studies of polymer blends exhibiting strong intermolecular interactions has been characterization of the morphology and thermal−mechanical properties of either single-phase materials or phase-separated blends following an arbitrary and usually poorly characterized thermal history. As a result, knowledge of the effect of strong intermolecular interactions on the phase separation process is limited. Our research seeks to answer the following questions: (1) does complexation perturb the kinetics of phase separation and (2) are there novel mechanisms that may provide opportunities for developing unique blend morphologies and application. This paper describes the effect of ion−dipole complexation on the miscibility and phase separation kinetics of polystyrene−polyamide blends and, in particular, on the kinetics of phase separation within the spinodal region of the phase diagram.

A number of studies of spinodal decomposition (SD) in polymer mixtures that do not exhibit strong intermolecular interactions have been reported.[4−13] The most extensively studied blend is polystyrene (PS) with poly(vinyl methyl ether) (PVME).[4−8] Light-scattering results for early-stage SD agree with Cahn−Hilliard theory,[14−16] which predicts a scattering peak corresponding to a dominant wavelength of the concentration fluctuations and an exponential growth of the scattering intensities. At later stages of SD, the scattering intensity deviates from exponential growth and has a power-law time dependence[8−10] as predicted by several other kinetic theories.[17−20]

The only report of the effect of specific intermolecular associations on the phase separation kinetics of a polymer blend was by He et al.,[21] who studied blends of poly(butyl methacrylate) with a polystyrene modified with 1.5 mol % of a hydroxy-containing comonomer. That system exhibits lower critical solution temperature (LCST) behavior, and miscibility occurs because of hydrogen bonding between the ester and hydroxyl groups. At lower phase separation temperatures, i.e., small excursions into the spinodal region, multiple structures developed in the blend which suggested that multiple mechanisms may be involved in the phase separation process. For most cases, however, the kinetics of phase separation followed Cahn−Hilliard theory in the early stage of spinodal decomposition and a self-similar mechanism in the later stages, similar to non-associating polymer blends such as PS/PVME.

The failure to observe an effect of a specific intermolecular interaction on SD kinetics in ref 21 may be a consequence of the low concentration of hydroxyl groups on the polystyrene, ca. five per chain, and the weakening of the hydrogen bond at the elevated temperatures used to study phase separation where the cross-link effect of hydrogen bonding may not be significant. At elevated temperatures, the association−dissociation equilibrium shifts toward nonassociated hydroxyl and ester groups. An objective of the present study was to utilize a polymer blend having a relatively higher degree of intermolecular association at the phase separation temperature and to investigate how physical cross-links affect the phase separation kinetics accompanying spinodal decomposition.

The polymers used in this study were the lithium salt of a lightly sulfonated polystyrene ionomer (Li-SPS) and an N-alkylated polyamide, poly(*N,N′*-dimethylethylene

[†] University of Connecticut.
[‡] National Institute of Standards and Technology.
[⊗] Abstract published in *Advance ACS Abstracts,* May 1, 1996.

S0024-9297(96)00074-5 CCC: $12.00

sebacamide). The latter is methylated nylon 2,10 and is hereafter referred to as mPA. The substitution of the methyl group for the amide proton prevents self-hydrogen bonding, which yields a relatively low melting temperature, ca. 75 °C, and very slow crystallization kinetics.[22] The low melting point provided the distinct advantage of having the melt state of the polyamide accessible at reasonably low experimental temperatures so that degradation of the polymers was not a crucial concern. The slow crystallization kinetics made it relatively easy to produce completely amorphous samples. Characterization of the Li^+−amide complex in Li-SPS/mPA blends is reported elsewhere.[23,24]

Experimental Details

Materials. Poly(*N*,*N*′-dimethylethylene sebacamide) (mPA) was prepared by a nucleophilic acyl substitution reaction following the procedure of Huang and Kozakiewicz.[22] The molecular weight averages determined by gel permeation chromatography using 1-methyl-2-pyrrolidinone as a solvent at room temperature were M_n = 25 000 and M_w = 65 000, referenced to a polystyrene calibration curve.

Free acid derivatives of lightly sulfonated polystyrene (H-SPS) were prepared by sulfonating a polystyrene homopolymer (M_w = 288 000, M_w/M_n = 2.7) in 1,2-dichloroethane at 50 °C using acetyl sulfate as the sulfonating reagent.[25] The sulfonation reaction adds sulfonic acid groups randomly to the para position of the styrene rings. The sulfonation level was determined by titration of H-SPS in a mixture solvent of 90% toluene/10% methanol with methanolic NaOH. Three samples with sulfonation levels of 4.0, 5.2, and 9.5 mol % (i.e., number of sulfonic acid groups per 100 styrene repeat units) were prepared, and the corresponding lithium salts were prepared by neutralizing the H-SPS in a 90% toluene/10% methanol solution with a 20% excess of a methanol solution of the lithium acetate. The Li-SPS ionomers were isolated from solution by steam stripping, filtered, washed, and dried under vacuum.

Samples of Li-SPS and mPA blends were prepared by mixing the two polymers in a solution of 10% methanol and 90% dichloroethane, filtering the solution through a 0.45 μm poly(tetrafluoroethylene) filter, and casting films onto glass microscope slides for cloud point and optical microscopy studies or onto quartz plates for time-resolved light-scattering measurements. In both cases, solution-cast films were dried in a vacuum oven for 2 days at temperatures below their respective phase separation temperatures and were then covered by another quartz plate (or a microscope cover slide) with a metal spacer between the two plates (or slides) to maintain the film thickness. The thickness of the specimen used for the light scattering was 0.1 mm, and that for cloud point or optical microscopy was 0.05 mm.

Cloud Point Measurements. Cloud point measurements were used to establish the phase boundaries for the Li-SPS/mPA blends. A Mettler FP80 microscope hot stage[26] was used to control the sample temperature at a constant heating rate, and a photodiode was used to monitor the light intensity at a 45° scattering angle as a function of the sample temperature. The cloud point was taken as the temperature at which the scattered light intensity deviated from the baseline as the temperature was increased. Cloud point data were obtained at two heating rates, 0.2 and 2 °C/min, and the phase transition temperature was calculated by a linear extrapolation of the two experimental cloud points to a temperature corresponding to zero heating rate.

Time-Resolved Light-Scattering Measurements. The kinetics of phase separation was studied by using a time-resolved light-scattering instrument at the National Institute of Standards and Technology (NIST). The experimental setup uses a 5 mW He−Ne laser as the incident beam and a set of neutral-density filters to keep the scattering intensity within the dynamic range of a one-dimensional photodiode array detector (Radicon tube). The sensitivity of the detector array was calibrated by fluorescence radiation from a nile blue dye (5×10^{-6} g/mL) embedded in gelatin. The collection, collimation, and angular mapping of scattering light were accomplished by a set of lenses, and an optical multichannel analyzer (OMA) was used for data acquisition.[5]

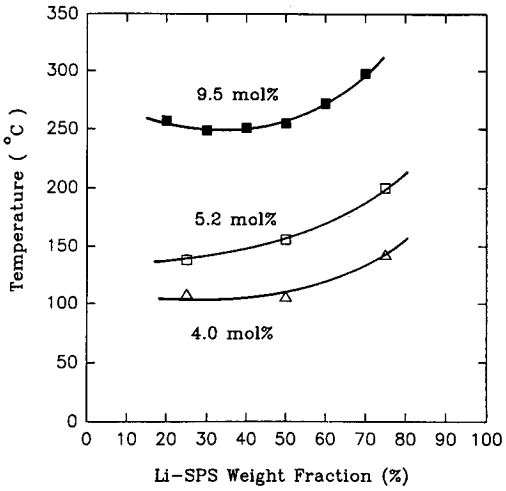

Figure 1. Cloud point curves of Li-SPS and mPA blends.

Two sets of heating blocks were used for the temperature control. The preheating block was used to anneal the sample at a temperature in the miscible region in order to bring the sample to a completely relaxed state, and the main block was set at the phase separation temperature. Both blocks are controlled by PID controllers to within ±0.02 °C.

The blend specimen was first annealed in the preheating block for several hours, and then phase separation was induced by quickly transferring the sample from the preheating block to the main block. Temperature equilibration in the main block took about 1 min.

Optical Microscopy Measurements. Optical micrographs were taken on a Zeiss transmission microscope with a Sony XC-77 CCD camera. The microscopic images were digitized using a frame grabber and software from Data Translation. A Mettler FP80 microscope hot stage was used to control the sample temperature during isothermal phase separation.

Results and Discussion

Liquid−Liquid Phase Diagrams. Cloud point curves determined for the Li-SPS/mPA blends as a function of sulfonation level and composition are given in Figure 1. PS and mPA are immiscible, and the introduction of the lithium sulfonate groups greatly enhances miscibility as a result of ion−dipole complexation.[23,24] Complete miscibility is achieved at room temperature with a sulfonation level as low as 4 mol %. The Li-SPS/mPA blends exhibit LCST phase behavior, and the critical point increased by ca. 150 °C when the sulfonation level was increased from 4 to 9.5 mol %.

De Gennes[27] predicted that intermolecular cross-links promote mixing of two polymers and that the enhancement of the one-phase region is directly proportional to the amount of cross-linking. In accordance with the de Gennes theory, experiments by Briber and Bauer[28] showed that cross-linking increased the single-phase region of the phase diagram of PS/PVME blends. Similarly, the phase diagrams shown in Figure 1 for the Li-SPS/mPA blends are also consistent with de Gennes's prediction in that the intermolecular ion−dipole complex may be viewed as a virtual, i.e., physical, cross-link. Unlike a covalent cross-link, a physical cross-link such as the ion−dipole complex is in equilibrium with the nonassociated metal sulfonate and amide groups and the relative populations are expected to be temper-

ature sensitive. At relatively low temperatures, e.g., at room temperature, the equilibrium favors the complex, so that the level of "cross-linking" is relatively high and the blend is miscible. As the temperature increases, however, the equilibrium of the Li^+−amide interaction shifts toward the nonassociated species, and the number of physical cross-links eventually falls below a critical value required to maintain miscibility and phase separation occurs. Increasing the sulfonation level is equivalent to increasing the absolute number of physical cross-links at all temperatures, so that the critical cross-link concentration is maintained to higher temperature. As a result, the LCST increases with increasing sulfonation of the ionomer.

Weiss and Lu[29] reported phase diagrams similar to Figure 1 for blends of SPS ionomers and poly(ϵ-caprolactam) (PA6) blends. In that case, the LCST depended on the cation used, and for a fixed sulfonation level and composition, the LCST increased as the cation was changed in the order of $Mg^{2+} \ll Li^+ < Zn^{2+} < Mn^{2+}$. Blends of the Na^+ salt of SPS and PA6 were immiscible. In a previous paper,[24] we showed that the strength of the ion−dipole complex in M-SPS/mPA blends increased in the order of $Li^+ < Cd^{2+} \leq Mn^{2+} < Cu^{2+} \leq Zn^{2+}$. Those results also appear to be consistent with the de Gennes prediction in that increasing the strength of the interaction should shift the ion−amide association equilibrium toward the complexed state, so that everything else being equal, the strongest ion−amide interaction should produce the highest LCST. The difference in the order of the LCST and strengths of the Mn^{2+} and Zn^{2+} salts in the SPS/PA6 and SPS/mPA systems is believed to arise from the different electronic environments of the amide nitrogen in the protonated and methylated polyamides.

In addition to the strong intermolecular associative interaction that occurs in the ionomer/polyamide blends, there is also a strong intramolecular repulsive interaction between the charged and uncharged portions of the ionomers.[30] The SPS ionomer may be viewed as a random copolymer of styrene and metal sulfonated styrene, and in light of contemporary theories of homopolymer/copolymer blends,[31−33] the intramolecular repulsions within the ionomer should also enhance miscibility with the polyamide. However, when blend miscibility arises from the "copolymer effect", upper critical solution temperature (UCST) phase behavior is usually observed. The fact that the phase diagrams in Figure 1 indicate LCST behavior suggests that the intermolecular cross-link effect is the dominant influence on phase behavior of Li-SPS/mPA blends; and in accordance with the de Gennes theory, we postulate that phase separation occurs when the number of physical cross-links falls below some critical value.

Phase Separation Kinetics. Experimental Results and Structure Pinning. A 50/50 (wt %) blend of mPA and the Li-SPS with a sulfonation level of 5.2 mol % was used to investigate the kinetics of phase separation. This blend had a cloud point of 156 °C, and isothermal time-resolved light-scattering measurements were carried out at two temperatures, 175 and 195 °C, that were chosen to be sufficiently greater than the cloud point so as to probably be within the spinodal region of the phase diagram.

Figure 2 shows scattering intensity vs wavevector, q ($q = 4\pi \sin\theta/\lambda$, where λ is the wavelength of the incident light and θ is one-half the scattering angle), at selected times after the Li-SPS/mPA blend underwent a temperature jump from 150 to 175 °C. The lines through the data in Figure 2 have no significance; they are merely to guide the eye. There are two important observations related to the evolution of the scattering profile in Figure 2: (1) the scattering intensities increased with time over the entire q range, which indicates that concentration fluctuations of various size scales were formed simultaneously during the process, and (2) the scattering intensities and the profile did not change significantly beyond the longest time shown in figure (122 min), which indicates that the growth of the phase-separated structure was retarded at long times and appeared to stall.

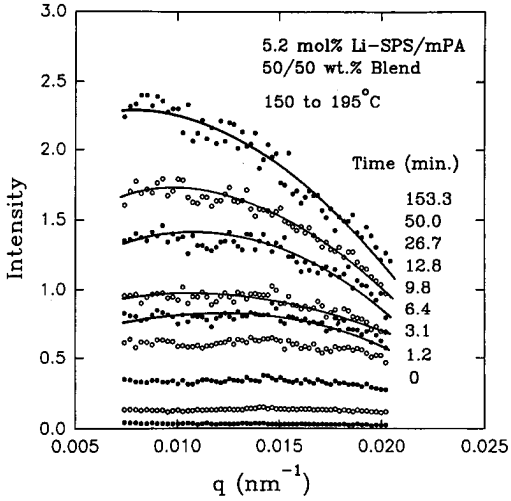

Figure 2. Time evolution of the isothermal light-scattering intensity vs wavevector for a 50/50 blend of 5.2 mol % Li-SPS and mPA following a temprature jump from 150 to 175 °C. The solid lines have no real significance and are intended to serve only as a guide for the observation.

The scattering profile of a polymer blend undergoing spinodal decomposition usually exhibits a distinctive peak at a constant q value at early stages of phase separation and the peak moves toward lower q at late stages of SD. The scattering peak characterizes a dominant concentration fluctuation or domain size.[8] The absence of a peak in Figure 2 indicates that no dominant domain size occurred, which is a departure from the usual SD. As will be discussed later in this section, the broad distribution of domain sizes may be related to the random distribution of the lithium sulfonate groups along the ionomer chains.

Figure 3 shows scattering profiles of the Li-SPS/mPA blend at various times following a temperature jump from 150 to 195 °C. As in Figure 2, the scattering intensities and profile did not change significantly beyond the longest time indicated in the figure, in this case, 153 min. A comparison of Figures 2 and 3 reveals two major differences in the structures of the blend at the two temperatures. The scattering profile, i.e., the structure factor, of the blend at the higher temperature, Figure 3, shows a significantly higher intensity and a steeper scattering profile with relatively higher intensity at lower q. Those two differences in the structure factor reflect an increase in the concentration gradient and in the domain sizes at the higher temperature, and they demonstrate that the phase separation temperature can be used as a variable to control the morphology of the blend.

The stalling of the phase separation process shown in Figures 2 and 3 is unusual. At both temperatures, the structure factor becomes nearly constant after 2−2.5

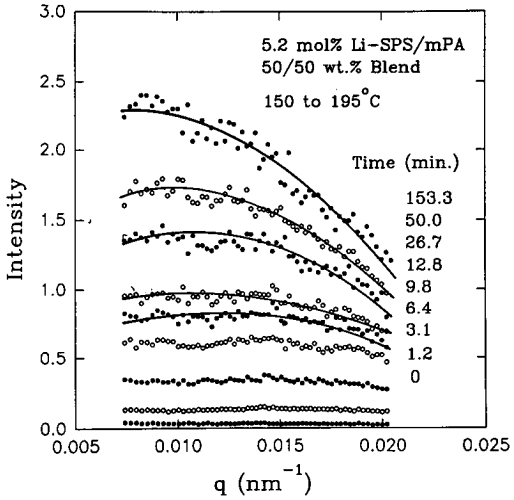

Figure 3. Time evolution of the isothermal light-scattering intensity vs wavevector for a 50/50 blend of 5.2 mol % Li-SPS and mPA following a temperature jump from 150 to 195 °C. The solid lines have no real significance and are intended to serve only as a guide for the observation.

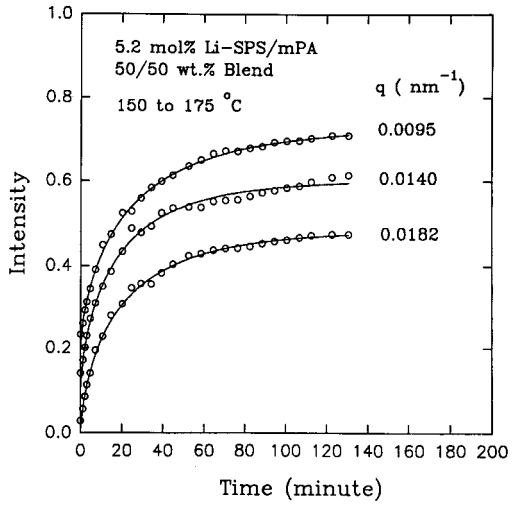

Figure 4. Light-scattering intensity at 175 °C vs time for three values of q for the experiment described in Figure 2.

h and scattering intensities at high q values remain comparable to those at low q values, which indicates the persistence of a significant amount of small domains. In normal SD, however, the phase-separated domains coalesce into larger ones at late stages of phase separation so as to reduce the interfacial energy. It is clear from Figures 2 and 3 that this is not the case in the Li-SPS/mPA blends, and some new mechanism acts to "pin" the morphology that was formed before the late stage of phase separation.

This pinning effect is better illustrated in plots of the scattering intensity vs time at constant q in Figures 4 and 5 for the phase separation at 174 and 195 °C, respectively. At both temperatures, the scattered light intensity at any q approaches an asymptotic value at long times. Even at early times, the growth of the scattered light intensity does not follow conventional Cahn−Halliard theory,[14−16] i.e., eq 1,

$$I(q,t) = I(q,0)\mathrm{e}^{2R(q)t} \qquad (1)$$

where q is the scattering vector, t is time, $I(q,t)$ is the scattering intensity, $I(q,0)$ is the initial scattering intensity, and $R(q)$ is the growth rate of the fluctuation with a wavevector q.

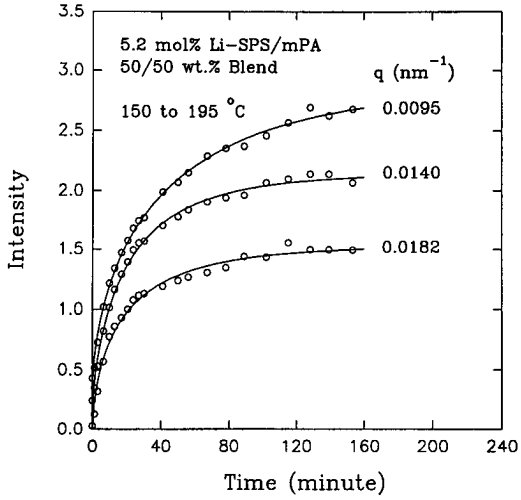

Figure 5. Light-scattering intensity at 195 °C vs time for three values of q for the experiment described in Figure 3.

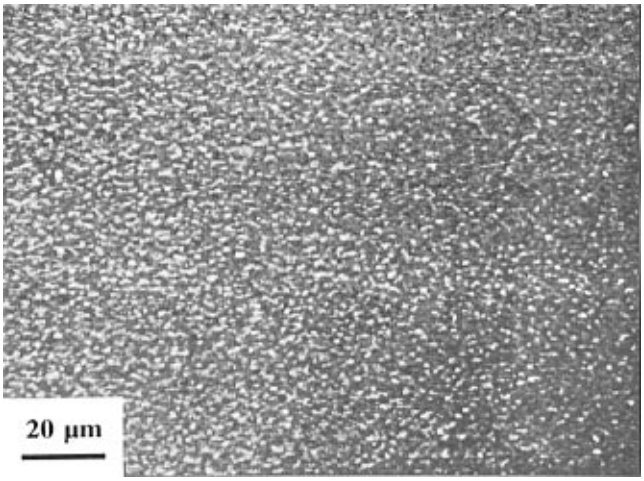

Figure 6. Optical micrograph of a 50/50 blend of 5.2 mol % Li-SPS and mPA after it was annealed at 175 °C for 2 h.

The data, however, obey the following equation over the entire experimental time scale:

$$I(q,t) = I_\infty(q)[1 - \mathrm{e}^{-(t/r_0)^\alpha}] \qquad (2)$$

The solid lines in Figures 4 and 5 represent the least squares fits of eq 2, and α ranges from 0.65 to 0.75. This growth behavior of the scattering intensity bears a striking resemblance to the structure growth in the spinodal decomposition of gelatin,[34] where phase separation does not go to completion because of gelation.

The structure pinning phenomenon was also directly observed by following the phase separation by optical microscopy. No structure was observed when a 50/50 blend of 5.2 mol % Li-SPS/mPA was annealed at 150 °C, a temperature within the miscible region. A phase-separated structure began to develop, however, when the temperature was jumped to 175 °C. Figure 6 shows a micrograph of the blend morphology after annealing at 175 °C for 2 h. Further annealing at this temperature did not notably change the structure, which is consistent with the SALS data. The phase-separated structure shown in Figure 6 has a spatial steric regularity, and there is a fairly broad distribution of domain sizes. The larger domain sizes are on the order of only 1 μm, which is much smaller than the typical domain size of a macrophase-separated binary polymer blend.

For example, for PVME/PS blends, phase-separated domain sizes are typically as large as 10−50 μm.[13]

Molecular Origin of Pinning. Glotzer et al.[35] developed a dynamic model of a phase-separating system in which nearest-neighbor monomers can interact with one of two distinct energies, e.g., van der Waals interaction and a stronger interaction. Using Monte Carlo simulations to study the nonequilibrium dynamics of phase separation, they showed that in the case where strong bonds form but rarely break, the system undergoing SD eventually forms a pinned, nonequilibrium, microphase-separated structure. Their model suggests that a random, strong interaction within one of the two resulting phases is responsible for the structure pinning.

In the phase separation of gelatin, where phase separation and gelation occur concurrently, Glotzer et al.[35] suggest that two different interaction energies are present in the system: (1) van der Waals interactions that are associated with the phase separation of the polymer from the solvent and (2) hydrogen bonding that controls the cross-linking of the chains. Competition between those two interactions pins the structure of the phase-separating mixture, because the formation of cross-linked gel between polymer chains arrests phase separation. It is important to note that in the gelatin system, the cross-linked gel is generated in the course of the phase separation process and is not initially present.

An argument similar to that for gelatin may be extended to the Li-SPS/mPA blend. The shift of the complex equilibrium at elevated temperatures toward nonassociated species initiates the phase separation process. Phase separation produces an ionomer-rich phase and a polyamide-rich phase. Two things may occur in the ionomer-rich phase. On the one hand, the stoichiometry of Li^+ ions to amide groups increases within this phase compared with the original single-phase melt which may produce sufficient physical cross-links between the ionomer and polyamide to effectively gel the ionomer-rich phase. On the other hand, if the ion−amide interaction is inhibited at the phase separation temperature, the increased concentration of lithium sulfonate groups in the ionomer-rich phase may result in microphase separation of the salt groups, which is common in bulk ionomers.[36] The microphase-separated ionic aggregates also act as physical cross-links and could gel the ionomer-rich phase. In either case, the lack of molecular mobility due to local gelation of the ionomer-rich phase may stall phase separation and pin the morphology. Of course, there is no real cross-link in the Li-SPS/mPA system. Both the ion−amide complexation and the ionic aggregation are in dynamic equilibrium with nonassociated and nonaggregated species. As a result, the "strong bonds" are continually breaking and re-forming and the relative time spent in each state is dictated by the equilibrium constant. The dynamic nature of the strong bond may still permit a slow continuation of phase separation. However, as the local concentration of strong bonds increases, the rate of the phase separation will become very slow and limited by the dynamics of the strong molecular associations.

When the phase separation temperature is increased, e.g., from 175 to 195 °C, both the ion−amide and ionic aggregate equilibria shift further toward nonassociated or nonaggregated species, and the phase separation process is allowed to proceed further before pinning occurs. That would explain the differences in the scattering profiles at the longer times in Figures 2 and 3.

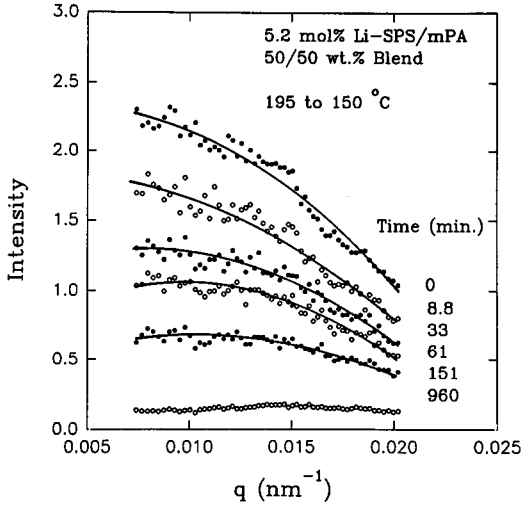

Figure 7. Time evolution of the isothermal light-scattering intensity vs wavevector for a 50/50 blend of 5.2 mol % Li-SPS and mPA following a temperature jump from 195 to 150 °C after first phase-separating at 195 °C. The solid lines have no real significance and are intended to serve only as a guide for the observation.

Within a given Li-SPS-rich domain, the local Li-SPS concentration may not be homogeneous throughout that domain, since the functional groups in Li-SPS chains are randomly distributed and the minimum Li-SPS concentration needed to achieve the local gelation depends on the sulfonation level within that particular domain. In other words, the extent of phase separation depends on the local sulfonation level, and neither a distinctive interphase nor a monodisperse ionic concentration in all the Li-SPS-rich microdomain is expected. This may explain the relatively flat scattering profiles in Figures 2 and 3 and the absence of a characteristic scattering peak.

Consistent with the results of Glotzer et al.[35] and of other similar model simulations,[37] the phase separation data for the Li-SPS/mPA blend do not exhibit a linear growth region at early times where the scattering intensity increases exponentially as predicted by Cahn−Hilliard theory. This may be due to the fact that the mixture was well inside the unstable region when phase separation was initiated after a temperature jump. In that case, the higher order terms of the Ginzburg−Landau equation may no longer be neglected[9] and, therefore, the linearized Cahn−Hilliard model is not valid.

Thermal Reversibility of Phase Separation. The reversibility of the phase behavior and phase separation shown in Figures 1 and 3 is demonstrated by the data in Figure 7, which show the evolution of the scattering profile after allowing a 50/50 blend of 5.2 mol % Li-SPS and mPA to first phase separate at 195 °C and then quenching the temperature to 150 °C, which is in the single-phase region of the phase diagram in Figure 1. The scattering intensities over the entire q range decreased with time, which indicates that remixing of the blend occurred at 150 °C. The remixing process was much slower than phase separation (cf. Figures 3 and 7), which is a consquence of the low mobility of the polymers at the lower temperature.

Conclusions

Blends of the lithium salt of lightly sulfonated polystyrene and poly(*N*,*N*′-dimethylethylene sebacamide)

(Li-SPS/mPA) are miscible as a result of strong ion−amide complexation. Complete miscibility at room temperature occurs with as little as 4 mol % sulfonation. The blends exhibit LCST phase behavior, and an increase of the sulfonation level from 4 to 9.5 mol % raises the critical temperature ca. 150 °C. The ion−amide complex acts essentially as an intermolecular cross-link, and the enhancement of miscibility with increasing sulfonation is consistent with de Gennes's prediction[27] that cross-linking increases the single-phase region of a partially miscible polymer blend.

Phase separation of the Li-SPS/mPA blends may be thermally induced and is thermodynamically reversible. The phase separation kinetics that occur following a temperature jump deep into the spinodal region of the phase diagram deviated from conventional Cahn−Hilliard theory,[14−16] and a structure pinning phenomenon similar to that reported for the spinodal decomposition of gelatin[34] was observed. The pinning, i.e., stalling of the phase separation process, is attributed to either concentrating ion−amide complexes in the ionomer-rich phase or the formation of microphase-separated ionic aggregates within the ionomer during phase separation. Either mechanism is expected to gel the ionomer-rich phase, and the lack of molecular mobility arrests the phase separation process. The extent of phase separation that occurred before pinning was temperature dependent. The structure pinning mechanism may be useful for controlling the development of a two-phase morphology, and it may have particular application in processing of polymer blends so as to achieve well-defined microstructures.

Acknowledgment. This research was supported by the Polymer Compatibilization Research Consortium at the University of Connecticut and by a grant from the Polymers Program of the National Science Foundation (Grant DMR 9400862). The authors thank Dr. Sanghoon Kim for help with the optical microscopy experiments.

References and Notes

(1) Matsuo, M.; Nozaki, C.; Jyo, Y. *Polym. Eng. Sci.* **1969**, *9*, 197.
(2) Olabisi, O.; Bobeson, L. M.; Shaw, M. T. In *Polymer−Polymer Miscibility*; Academic Press: New York, 1979.
(3) For example: (a) Lu, X.; Weiss, R. A. *Macromolecules* **1991**, *24*, 4381; (b) Lu, X.; Weiss, R. A. *Macromolecules* **1992**, *25*, 6185; (c) Molnar, A.; Eisenberg, A. *Macromolecules* **1992**, *25*, 5774; (d) Molnar, A.; Eisenberg, A. *Polymer* **1991**, *32*, 370; (e) Ng, C. W. A.; Bellinger, M. A.; MacKnight, W. J. *Macromolecules* **1994**, *27*, 6942.
(4) Okada, M.; Han, C. C. *J. Chem. Phys.* **1986**, *85*, 5317.
(5) Sato, T.; Han, C. C. *J. Chem. Phys.* **1988**, *88*, 2057.
(6) Hashimoto, T.; Sasaki, K.; Kawai, H. *Macromolecules* **1984**, *17*, 2812.
(7) Hashimoto, T.; Itakura, M.; Hasegawa, H. *J. Chem. Phys.* **1986**, *85*, 6118.
(8) Hashimoto, T. In *Current Topics in Polyer Science, II*; Ottenbrite, Utracki, Inoue, Eds.; Hanser: Munich, Vienna, New York, 1987.
(9) Hashimoto, T. *Phase Transitions* **1988**, *12*, 47.
(10) Kyu, T.; Saldanha, J. M. *Macromolecules* **1988**, *21*, 1021.
(11) MacMaster, L. P. *Adv. Chem. Ser.* **1975**, *142*, 43.
(12) Nojima, S.; Nose, T. *Polym. J.* **1982**, *14*, 907.
(13) Davis, D. D.; Kwei, T. K. *J. Polym. Sci., Polym. Phys. Ed.* **1980**, *18*, 2337.
(14) Cahn, J. W.; Hilliard, J. E. *J. Chem. Phys.* **1958**, *28*, 258.
(15) Cahn, J. W.; Hilliard, J. E. *J. Chem. Phys.* **1959**, *31*, 688.
(16) Cahn, J. W. *J. Chem. Phys.* **1965**, *42*, 93.
(17) Kawasaki, K.; Ohta, T. *Prog. Theor. Phys.* **1978**, *59*, 362.
(18) Furukawa, H. *Physica A (Amsterdam)* **1984**, *123A*, 497.
(19) Siggia, E. D. *Phys. Rev. A* **1979**, *43*, 1733.
(20) Lifshitz, I. M.; Slyozov, V. V. *J. Phys. Chem. Solids* **1961**, *19*, 35.
(21) He, M.; Liu, Y.; Feng, Y.; Jiang, M.; Han, C. C. *Macromolecules* **1991**, *24*, 464.
(22) Huang, S. J.; Kozakiewicz, J. *J. Macromol. Sci., Chem.* **1981**, *A15*, 821.
(23) Feng, Y., Ph.D. Thesis, University of Connecticut, 1995.
(24) Feng, Y.; Schmidt, A.; Weiss, R. A *Macromolecules* **1996**, *29*, 3909.
(25) Makowski, H. S.; Lundberg, R. D.; Singhal, G. H. U.S. Patent, 3,870,841, 1975.
(26) Certain commercial materials and equipment are identified in this paper in order to specify adequately the experimental procedure. In no case does such identification imply recommendation or endorsement by the National Institute of Standards and Technology, nor does it imply necessarily the best available for the purpose.
(27) de Gennes, P. G. *J. Phys. Lett.* **1979**, *40*, 69.
(28) Briber, R. M.; Bauer, B. J. *Macromolecules* **1988**, *21*, 3296.
(29) Weiss, R. A.; Lu, X. *Polymer* **1994**, *34*, 1963.
(30) Beck Tan, N. C.; Liu, X.; Briber, R. M.; Peiffer, D. G. *Polymer* **1995**, *36*, 1969.
(31) ten Brinke, G.; Karasz, F. E.; MacKnight, W. J. *Macromolecules* **1983**, *16*, 1827.
(32) Kambour, R. P.; Bendler, J. T.; Bopp, R. C. *Macromolecules* **1983**, *16*, 753.
(33) Paul, D. R.; Barlow, J. W. *Polymer* **1984**, *25*, 487.
(34) Bansil, R.; Lal, J.; Carvalho, B. L. *Polymer* **1994**, *33*, 2961.
(35) Glotzer, S. C.; Gyure, M. F.; Sciortino, F.; Coniglio, A.; Stanley, H. E. *Phys. Rev. E* **1994**, *49*, 247.
(36) Eisenberg, A.; King, M. *Ion-Containing Polymers*; Academic Press: New York, 1977.
(37) Grest, G.; Srolovitz, D. J. *Phys. Rev. Lett.* **1985**, *32*, 3014.

MA960074O